

## Article

# Influence of Juvenile Growth on Xylem Safety and Efficiency in Three Temperate Tree Species

Manish Kumar <sup>1,2</sup> , Pierre-André Waite <sup>1</sup>, Sharath Shyamappa Paligi <sup>1,3</sup> and Bernhard Schuldt <sup>1,\*</sup> 

<sup>1</sup> Ecophysiology and Vegetation Ecology, Julius-von-Sachs-Institute of Biological Sciences, University of Würzburg, Julius-von-Sachs-Platz 3, 97082 Würzburg, Germany; manish.kumar@uni-wuerzburg.de (M.K.); pierre-andre.waite@uni-wuerzburg.de (P.-A.W.); sharath.paligi@uni-goettingen.de (S.S.P.)

<sup>2</sup> ICAR—Central Soil Salinity Research Institute (CSSRI), Karnal 132001, India

<sup>3</sup> Plant Ecology and Ecosystems Research, Albrecht von Haller Institute for Plant Sciences, University of Göttingen, 37073 Göttingen, Germany

\* Correspondence: bernhard.schuldt@plant-ecology.de

**Abstract:** The evolution of the internal water transport system was a prerequisite for high plant productivity. In times of climate change, understanding the dependency of juvenile growth on xylem hydraulic physiology is therefore of high importance. Here, we explored various wood anatomical, hydraulic, and leaf morphological traits related to hydraulic safety and efficiency in three temperate broadleaved tree species (*Acer pseudoplatanus*, *Betula pendula*, and *Sorbus aucuparia*). We took advantage of a severe natural heat wave that resulted in different climatic growing conditions for even-aged plants from the same seed source growing inside a greenhouse and outside. Inside the greenhouse, the daily maximum vapour pressure deficit was on average 36% higher than outside during the growing seasons. Because of the higher atmospheric moisture stress, the biomass production differed up to 5.6-fold between both groups. Except for one species, a high productivity was associated with a high hydraulic efficiency caused by large xylem vessels and a large, supported leaf area. Although no safety-efficiency trade-off was observed, productivity was significantly related to  $P_{50}$  in two of the tree species but without revealing any clear pattern. A considerable plasticity in given traits was observed between both groups, with safety-related traits being more static while efficiency-related traits revealed a higher intra-specific plasticity. This was associated with other wood anatomical and leaf morphological adjustments. We confirm that a high hydraulic efficiency seems to be a prerequisite for a high biomass production, while our controversial results on the growth–xylem safety relationship confirm that safety-efficiency traits are decoupled and that their relationship with juvenile growth and water regime is species-specific.

**Keywords:** hydraulic efficiency; biomass; growth rate; hydraulic variability; phenotypic plasticity; safety-efficiency trade-off; vulnerability curve



**Citation:** Kumar, M.; Waite, P.-A.; Paligi, S.S.; Schuldt, B. Influence of Juvenile Growth on Xylem Safety and Efficiency in Three Temperate Tree Species. *Forests* **2022**, *13*, 909. <https://doi.org/10.3390/f13060909>

Received: 4 May 2022

Accepted: 6 June 2022

Published: 10 June 2022

**Publisher's Note:** MDPI stays neutral with regard to jurisdictional claims in published maps and institutional affiliations.



**Copyright:** © 2022 by the authors. Licensee MDPI, Basel, Switzerland. This article is an open access article distributed under the terms and conditions of the Creative Commons Attribution (CC BY) license (<https://creativecommons.org/licenses/by/4.0/>).

## 1. Introduction

Worldwide, trees in forested ecosystems are increasingly exposed to drought and heat stress due to the rise in intensity and frequency of global change-type drought events [1]. Thereby, prolonged drought exposure may affect plant productivity and biomass allocation [2], survival [3,4], and potentially future species abundance and distributions [5]. During drought exposure, plants close their stomata to maintain high xylem water potentials and to reduce transpirational water loss [6]. However, prolonged drought conditions might ultimately lead to hydraulic failure because of continuous residual water loss via the cuticle and bark [7]. Under severe and prolonged water stress, xylem tensions therefore ultimately reach critical thresholds causing water-filled vessels to embolize, which disrupts the continuous water column and ultimately causes plant death [8–10]. Thus, the likelihood of hydraulic failure and xylem characteristics are supposed to be highly interconnected.

The ability to resist embolism formation is mainly depicted by the water potential at a 50% loss of conductivity ( $P_{50}$ ) and referred to as hydraulic safety. Although it is meanwhile well-established that pit membrane thickness is directly related to the  $P_{50}$ -value [11,12], wide vessels have likewise commonly been associated with low hydraulic safety, both within [13,14] and across species [15,16]. Therefore, species with thin pit membranes and large vessels may be more vulnerable to water stress-induced cavitation [17]. However, large vessels are directly linked to the maximal capacity of the xylem to transport water, i.e., the xylem-specific hydraulic conductivity ( $K_S$ ; hereafter ‘hydraulic efficiency’), which scales to the fourth power of conduit diameter.

Hence, a trade-off between hydraulic efficiency and safety has traditionally been hypothesized [18–20]. Both a high hydraulic efficiency and a high safety, are advantageous for plant growth and drought-tolerance. However, because of their contrasting anatomical needs, both are supposedly not achievable by the same species, and natural selection is expected to drive species towards one extreme or another [20,21]. In fact, empirical evidence is ambiguous, and a majority of recent studies could find only weak or no relations between hydraulic efficiency and safety in trees [14,15,20,22,23]. Most likely, such a safety–efficiency trade-off depends on a range of wood anatomical properties and not just vessel diameter [24]. Accordingly, hydraulic safety–efficiency relationships are more likely to appear in interspecific studies with species from different habitats than in samples of co-occurring, phylogenetically related taxa or in intraspecific studies.

Although safety–efficiency trade-offs are scale-dependent, the water status of plants is highly related to xylem characteristics, and xylem physiology has been termed the backbone of terrestrial plant productivity because of the close connection between carbon uptake and water release via the stomata [25]. This is in line with [26], hypothesizing that high productivity should be closely associated with a high hydraulic efficiency. In the case of a safety–efficiency trade-off, this might mean that productive trees favour hydraulic efficiency over safety to ensure high growth rates. Since then, a plausible link between stem growth rate and hydraulic efficiency and safety has been tested empirically revealing close, yet contrasting, associations [27–32]. For example, no relationship between growth and hydraulic efficiency was found in *Populus nigra* across different genotypes at the intra-population level [33]. Nonetheless, relations between productivity and hydraulic efficiency seem to be closely related to plant water transport capacity and therefore wood anatomical features such as a large vessel diameter [34–37]. On the other hand, xylem safety may also decline with an increasing growth rate. Firstly, due to the anticipated trade-off between hydraulic safety and efficiency, but also because of carbon allocation conflicts. In plants, assimilated carbon might either be allocated to cell walls to resist the higher hydraulic tensions [25] or to foliar and axial tissues for a higher productivity [28]. However, most studies did not observe any relationship between hydraulic safety and growth [14,33,38–40] although exceptions exist [35,41].

In view of current and future climate change impacts on the Central European forests, the selected minor timber tree species—Sycamore maple (*Acer pseudoplatanus*), European rowan (*Sorbus aucuparia*), and Silver birch (*Betula pendula*)—are ecologically important because of their different habitat preferences [42], highlighting their potential suitability for the establishment of climate-resilient forests.

In order to test whether differences in juvenile growth affect xylem efficiency and/or safety, we measured 17 structural, functional, and hydraulic traits in evenly-aged young trees differing up to 5.6-fold in biomass production, which was induced by different climatic growing conditions during an exceptional heat wave in the year 2019. We analysed the association of structural parameters and hydraulic safety–efficiency traits as well as other functional traits linked to resource acquisition and partitioning. We studied interactions across and within species including the plastic response of the plants to contrasting growing conditions. We asked whether (i) a low hydraulic safety ( $P_{50}$ ) and a high hydraulic efficiency ( $K_S$ ) are associated with high juvenile growth rates, (ii) a trade-off exists between hydraulic

safety and efficiency in seed-grown saplings, and whether (iii) hydraulic safety–efficiency traits are related to xylem anatomy.

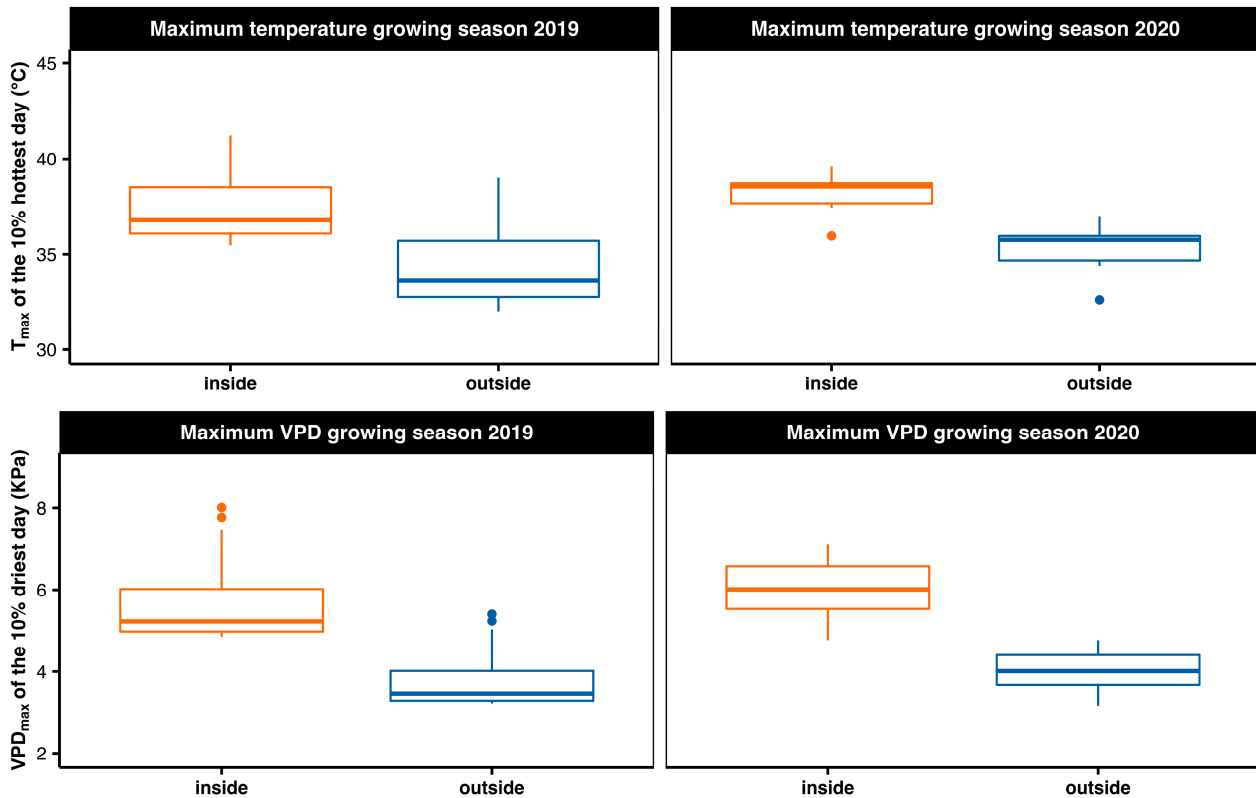
## 2. Material and Methods

### 2.1. Study Site, Microclimatic Measurements, and Plant Material

The present study was conducted at the Chair of Ecophysiology and Vegetation Ecology, Julius-von-Sachs-Institute of Biological Sciences, Würzburg, Germany (180 m a.s.l.; mean annual temperature: 10 °C; mean annual precipitation: 625 mm). From seeds collected in the Botanical Garden Würzburg in 2018, we grew 82 plants of three temperate deciduous angiosperm species, namely *Acer pseudoplatanus* (ACPS), *Betula pendula* (BEPE), and *Sorbus aucuparia* (SOAU) for 18 months. These three tree species were selected because of their anticipated differences in growth performance and hydraulic traits. *B. pendula* is a typical pioneer, broad-leaved tree species in the temperate and boreal forests of Europe. It has the ability to grow in both wet and dry habitats but has high needs for light. It can survive under fairly extreme conditions through physiological adaptation and is considered to follow an isohydric stomatal control strategy [43]. The second species selected, *A. pseudoplatanus*, prefers a humid climate, high rainfall, and moderately moist to wet site up to 1800 m elevation. The species has a high water demand and needs large rooting space. The species is considered as moderately drought and heat sensitive [44] and is defined as isohydric [45]. The last species of our sample, *S. aucuparia*, occurs as a tree or a shrub and can experience wide water potential variations during droughts (i.e., related to an anisohydric behavior), and shows a high resistance to cavitation [46]. In the Botanical Garden, open-field air temperature and air humidity is continuously measured at 2 m height aboveground (Umweltmeßtechnik Adolf Thies GmbH & Co. KG, Göttingen, Germany). Micro-climatic conditions inside the growing chamber of the greenhouse are likewise continuously recorded (RAM GmbH Mess-und Regeltechnik, Herrsching, Germany), but unfortunately the data for the 2019 and 2020 growing seasons were lost due to a fatal computer crash. We therefore used the data from the 2021 growing season, which also became a dry and warm growing season in Würzburg, to model the microclimatic conditions in 2019 and 2020 (Figures S1 and S2); both were highly interrelated according to a linear model ( $R^2 = 0.85$ ,  $p < 0.001$ ; data not shown).

After initial sowing in March 2019 and transplanting in May 2019, the seedlings were grown in 7.5 L pots in an Euroham soil mixture (Eurohum Faser, Article no. 12-03200-xx) containing N, P, K in a proportion of 14, 16, and 18 kg m<sup>-3</sup>, respectively. For the duration of the growing phase (i.e., 18 months), a subset of randomly selected 10 to 12 plants per species ( $n = 34$ ) were placed in a small chamber of a greenhouse with an area of 18 m<sup>2</sup>, hereafter named ‘inside’ or ‘stress treatment’. We took advantage of the severe climatic conditions in 2019, an unprecedented heat and drought event since more than 250 years [47], which exposed these plants to stressful environmental conditions resulting in reduced growth rates. This stress was mainly caused by high temperatures and high atmospheric moisture stress inside the growing chamber (Figure 1). Meanwhile, the remaining 14 to 18 plants per species ( $n = 48$ ) were grown outside under a transparent roof but with completely open sites, enabling air exchange due to wind, hereafter named ‘outside’ or ‘control treatment’. These plants were therefore exposed to more natural environmental conditions. As a consequence of the different growing locations, saplings that were grown inside the greenhouse chamber were strongly affected by the heat wave (i.e., stress treatment) while the plants outside experienced more natural growing conditions (control treatment), which was mirrored in large differences in growth rates. During the growing season in 2019, the daily maximum temperature ( $T_{\max}$ ) differed on average by 15.9% between inside and outside (mean  $\pm$  SE:  $29.5 \pm 0.4$  °C versus  $24.8 \pm 0.5$  °C), and vapour pressure deficit ( $VPD_{\max}$ ) differed by 36.2% ( $3.04 \pm 0.12$  kPa versus  $1.94 \pm 0.08$  kPa). Similar differences were observed during the growing season in 2020, where  $T_{\max}$  differed by 15.8% ( $29.7 \pm 0.3$  °C versus  $25.0 \pm 0.4$  °C) and VPD by 36.0% ( $3.08 \pm 0.10$  kPa versus  $1.97 \pm 0.07$  kPa). During the 10% of the hottest days in 2019 and 2020, a daily  $VPD_{\max}$  of

$5.89 \pm 0.27$  kPa or  $5.64 \pm 0.23$  kPa was reached inside the greenhouse, indicative for severe atmospheric moisture stress. Average outside values stayed below 4 kPa ( $3.93 \pm 0.19$  kPa in 2019 and  $3.75 \pm 0.16$  kPa in 2020, respectively; Figure 1).



None of the plants inside the greenhouse showed signs of leaf discoloration, indicating that frequent stomatal closure due to a high evaporative demand explains observed differences in biomass production as all other growing conditions were comparable (e.g., light exposure, soil composition and volume, and irrigation schedule). Please note that the plant material from both groups was even-aged and seeds originated from the same parental trees. After 18 months of growth under the different conditions, we collected plant material for structural, functional, and hydraulic measurements in August 2020.

## 2.2. Sample Collection, Structural Measurements, and Growth Rate

Before the hydraulic measurements, saplings were watered overnight to ensure full turgor and a relaxed state to minimize measurement artefacts associated with cutting under tension.

We performed all measurements on the main shoot of most saplings (i.e., structural measurements were performed on all 82 trees, while hydraulic and leaf morphological measurements were carried out on a subset of 57 to 64 trees including side branches (see Table S1 for more details). We first measured structural parameters of each sapling, i.e., the root collar diameter (RCD) and shoot length, and then proceeded to cut-off the main shoot at the root collar and to recut it under water several times in order to relax the xylem, thereby avoiding measurement artefacts associated with sample excision [48]. On this

shoot, we labelled a targeted segment to be used for hydraulic measurements, and collected and separated (i.e., divided in two groups: basal and apical leaves) all leaves above and below the proximal end of the targeted section and stored them in plastic bags at 4 °C until scanning. Furthermore, the distance from the segment used for hydraulic and wood anatomical measurements to the tip was recorded. Directly below the proximal end of the targeted segment, we stored a ~3 cm segment in 70% ethanol for subsequent wood anatomical analyses. After hydraulic measurements, the segment used and the remaining woody samples were oven-dried at 70 °C for 72 h. Subsequently, total aboveground biomass (AGB, g) was estimated by adding the total leaf dry mass per plant, and aboveground biomass increment (ABI, mg d<sup>-1</sup>) estimated by dividing AGB by the growth period, i.e., the difference between seed sowing and sapling harvesting time. A list of all traits measured with the corresponding acronyms and units is given in Table 1.

**Table 1.** List of variables included in this study with their definitions and units.

Abbreviation	Units	Definitions
<i>Growth attributes</i>		
RCD	mm	Collar diameter of the stem above the ground
Shoot length	cm	Shoot length from ground to uppermost leaf
AGB	g	Aboveground biomass
ABI	mg d <sup>-1</sup>	Aboveground biomass increment
<i>Hydraulic traits</i>		
$P_{12}$	MPa	Xylem pressure at 12% loss of hydraulic conductance
$P_{50}$	MPa	Xylem pressure at 50% loss of hydraulic conductance
$P_{88}$	MPa	Xylem pressure at 88% loss of hydraulic conductance
$K_S$	kg m <sup>-1</sup> MPa <sup>-1</sup> s <sup>-1</sup>	Specific conductivity
$K_L$	10 <sup>-4</sup> kg m <sup>-1</sup> MPa <sup>-1</sup> s <sup>-1</sup>	Leaf-specific conductivity
$K_{pit}$	kg m <sup>-1</sup> MPa <sup>-1</sup> s <sup>-1</sup>	Pit conductivity
$K_p$	kg m <sup>-1</sup> MPa <sup>-1</sup> s <sup>-1</sup>	Potential conductivity
<i>Foliar traits</i>		
HV	10 <sup>-4</sup> m <sup>2</sup> m <sup>-2</sup>	Huber value, i.e. the sapwood-to-leaf area ratio
$A_{leaf}$	cm <sup>2</sup>	Mean leaf size
SLA	cm <sup>2</sup> g <sup>-1</sup>	Specific leaf area
<i>Anatomical traits</i>		
$D$	µm	Mean vessel diameter
$D_h$	µm	Hydraulically weighted mean vessel diameter
VD	n mm <sup>-2</sup>	Vessel density
$A_{lumen}:A_{xylem}$	%	Lumen-to-sapwood area ratio

### 2.3. Leaf Traits

All leaves from basal and apical group (see the previous section for details) were scanned separately with an A3 high-resolution scanner (Expression 12000XL, EPSON, Nagano, Japan). We divided the leaves into two groups to relate hydraulic conductivity measurements to the leaf area that is supported by the measured segment (i.e., apical group). We then computed the areas to obtain total leaf area ( $A_L^{total}$ , cm<sup>2</sup>) and mean leaf area ( $A_{leaf}$ , cm<sup>2</sup>) per sapling using the ImageJ software. The Huber value (HV, 10<sup>4</sup> m<sup>2</sup> m<sup>-2</sup>), i.e., the sapwood-to-leaf-area ratio, was calculated by dividing the sapwood area (i.e., obtained from anatomical cross-sections) by the distal leaf area. All leaves were then oven-dried at 70 °C for 48 h to calculate specific leaf area (SLA, cm<sup>2</sup> g<sup>-1</sup>).

#### 2.4. Hydraulic Conductivity

In the laboratory, stem segments were shortened under water (mean length  $\pm$  SD:  $307.3 \pm 2.07$  mm), lateral branches cut off, and scars sealed with quick-drying contact adhesive (Loctite 431 with Loctite activator SF 7452, Henkel, Düsseldorf, Germany). Segment diameters were measured twice at the basal and distal ends of the segment and four times along the segment (mean diameter  $\pm$  SD:  $8.30 \pm 0.79$  mm). Subsequently, the bark was removed at the basal end and segments connected to the Xylem apparatus (Bronkhorst France, Montigny les Cormeilles, France) to measure hydraulic conductivity ( $K_h$ ;  $\text{kg m MPa}^{-1} \text{s}^{-1}$ ). We used filtered ( $0.2 \mu\text{m}$ ) and degassed demineralized water mixed with 10 mM KCl and 1 mM  $\text{CaCl}_2$ . We initially measured the actual hydraulic conductivity ( $K_h^{\text{act}}$ ) at a low pressure of 6 kPa and then measured maximum hydraulic conductivity ( $K_h^{\text{max}}$ ) after repetitively water-flushing the segments at a high pressure of 120 kPa for 10 min until  $K_h$  remained constant. The hydraulic conductivity and flow rate data were analyzed with the software XylWin 3.0 (Bronkhorst France, Montigny les Cormeilles, France). We calculated sapwood-specific hydraulic conductivity ( $K_S$ ;  $\text{kg m}^{-1} \text{MPa}^{-1} \text{s}^{-1}$ ) by dividing  $K_h^{\text{max}}$  with the basal sapwood cross-sectional area without pith and bark [14,24]. We also calculated leaf-specific hydraulic conductivity ( $K_L$ ;  $\text{kg m}^{-1} \text{MPa}^{-1} \text{s}^{-1}$ ) by dividing  $K_h^{\text{max}}$  by the supported leaf area.

#### 2.5. Vulnerability Curves

The flow-centrifuge technique [49] was used to construct xylem vulnerability curves (VCs) of the same stem segments used for hydraulic conductivity measurements. The samples were shortened to a length of ca. 27 cm and the bark was removed at both ends and had a basal diameter of  $7.91 \pm 0.09$  mm and an apical diameter of  $6.57 \pm 0.09$  mm (mean  $\pm$  SD). The segments were then inserted into a custom-made Cavitron rotor chamber attached to a centrifuge (Cavitron device built from a Sorvall RC-5C series centrifuge, customised) and measurements were made using the Cavisoft software (Cavisoft version 5.2.1, University of Bordeaux, Bordeaux, France).

Measurements started at a xylem pressure of  $-0.37$  MPa for *B. pendula*, and  $-0.83$  MPa for *A. pseudoplatanus* and *S. aucuparia*. We then stepwise raised the rotation speed corresponding to 0.2–0.3 MPa until the percentage loss of hydraulic conductivity (PLC) reached at least 90%. By plotting PLC against xylem pressure ( $\Psi_x$ ), vulnerability curves were generated for each branch. We used an exponential-sigmoidal function provided by [50] to derive the  $\Psi_x$  causing 50% loss of conductivity ( $P_{50}$ ):

$$\text{PLC} = 100 / (1 + \exp(s/25 \times (P_i - P_{50}))),$$

with  $s$  ( $\% \text{MPa}^{-1}$ ) being slope of the curve at  $P_{50}$  and  $P_i$ , the applied xylem pressure. Subsequently, the  $\Psi_x$  at 12% and 88% loss of conductivity ( $P_{12}$  and  $P_{88}$ ) were obtained by following [27] as:  $P_{12} = P_{50} - 50/s$  and  $P_{88} = P_{50} + 50/s$ . Values of  $P_{12}$  and  $P_{88}$  represent the thresholds of xylem tension at the onset and offset of cavitation, respectively.

#### 2.6. Wood Anatomy

A sliding microtome (G.S.L.1, Schenkung Dapples, Zürich, Switzerland) was used to cut three transverse sections of 10–20  $\mu\text{m}$  thickness from ethanol-stored segments. Sections were stained with safranin alcian blue (1% safranin in ethanol), rinsed with distilled water and ethanol (95%), and permanently embedded on glass slides using Euparal (Carl Roth, Karlsruhe, Germany). Slides were oven-dried at  $50^\circ\text{C}$  for ten days. Complete cross-sections were digitalized at 100x magnification with a resolution of 1.33 pixels  $\mu\text{m}^{-1}$  using a stereo-microscope equipped with an automatic stage and a digital camera (Observer.Z1, Carl Zeiss MicroImaging GmbH, Jena, Germany; Software: AxioVision c4.8.2, Carl Zeiss MicroImaging GmbH). The digitalized images were then analyzed using GIMP (version 2.10.14) and ImageJ (Version 1.51h) for anatomical traits using the particle analysis function. The recorded parameters include sapwood area ( $A_{\text{xylem}}$ ,  $\mu\text{m}^2$ ), lumen-to-sapwood area ratio

( $A_{\text{lumen}}:A_{\text{xylem}}$ , %), vessel density (VD,  $\text{n mm}^{-2}$ ), and vessel diameter ( $D$ ,  $\mu\text{m}$ ) from major (a) and minor (b) vessel radii using the equation,  $D = ((32 \times (a \times b)^3)/(a^2 + b^2))^{1/4}$  [51].  $D$  was then used to obtain the hydraulically-weighted vessel diameter ( $D_h$ ,  $\mu\text{m}$ ) according to [52] as  $D_h = \Sigma D^5/\Sigma D^4$ . Standardized  $D_h$  was calculated according to [53] as  $D_h^{\text{std}} = D_h/L^b$ , where  $L$  is the distance of the segment to the apex and  $b$  is the exponent constant (0.2) according to the metabolic scaling theory [54]. The potential conductivity ( $K_p$ ;  $\text{kg m}^{-1} \text{MPa}^{-1} \text{s}^{-1}$ ) was derived using the Hagen–Poiseuille equation:

$$K_p = \pi \times p \times \Sigma D^4 / (128 \times \eta \times A_{\text{xylem}}),$$

where  $\eta$  is the viscosity ( $1.002 \times 10^{-9}$  MPa s) and  $p$  the density of water ( $998.2 \text{ kg m}^{-3}$ ), both at  $20^\circ\text{C}$ , and  $A_{\text{xylem}}$  ( $\text{mm}^2$ ) is the analysed sapwood area. Pit conductivity was estimated as  $K_{\text{pit}} = ((1/K_s) - (1/K_p))^{-1}$  [55]. A low  $K_{\text{pit}}$  indicates that higher resistance to water flow has to be overcome.

### 2.7. Statistical Analyses

All statistical analyses were carried out with R version 4.0.3 [56] in the framework of the tidyverse package [57]. First descriptive statistics were applied, and then data were tested for normal distribution with a Shapiro–Wilk normality test. For inferential statistics, significant differences were tested by adopting a t-test or welch test within species as per treatment basis. However, Wilcoxon test was performed if normality assumptions were not met. We also performed linear models to test the effect of predictors on target variables, e.g., effect of growth rate on hydraulic traits. We log transformed variables that did not meet normality assumptions.

## 3. Results

### 3.1. Growth and Structural Differences across Species and Treatments

Because the species were monitored from seed sowing, the juvenile growth performance could be assessed in terms of shoot length and aboveground biomass increment per day (i.e., growth rate). For all species, we recorded significantly different growth-related parameters ( $p < 0.001$ ) between the control and stressed treatment (Figure 2, Table S1). All control plants had a higher growth compared to the stressed plants. In *B. pendula*, *A. pseudoplatanus*, and *S. aucuparia*, the shoot length was smaller in the stress treatment than in the control and differed by 47%, 50%, and 33%, respectively. For the aboveground biomass increment (ABI), the differences were even more pronounced and differed on average 2.8- to 5.3-fold between the control and stress treatment, i.e.,  $287 \text{ mg d}^{-1}$  versus  $61 \text{ mg d}^{-1}$  for *A. pseudoplatanus*,  $424 \text{ mg d}^{-1}$  versus  $79 \text{ mg d}^{-1}$  for *B. pendula*, and  $324 \text{ mg d}^{-1}$  versus  $117 \text{ mg d}^{-1}$  for *S. aucuparia* (Figure 2, Table S1).

### 3.2. Effects of Climatic Stress on Hydraulic, Wood Anatomical, and Leaf Morphological Traits

We found significant, yet contrasting, intra-specific differences between trees grown under stressed and optimal control conditions. Notably,  $P_{50}$  was more negative (i.e., higher resistance) in stressed *S. aucuparia* compared to the control (Figure 3a;  $p < 0.01$ ), while for *B. pendula*, we found that stressed plants were slightly less resistant to embolism formation ( $p < 0.05$ ). We did not find differences in hydraulic safety between the two groups of *A. pseudoplatanus*. Likewise, we found that hydraulic efficiency (i.e., specific conductivity,  $K_s$ ) was significantly higher in optimally-grown saplings of two of the three species (Figure 3b; *B. pendula* and *A. pseudoplatanus*) while the last one (*S. aucuparia*) showed no significant difference (Figure 3b); similar trends were found for  $K_{\text{pit}}$  (Figure S3). These differences in hydraulic efficiency were mirrored by xylem anatomical differences between groups as we found wider vessels in controlled plants of *A. pseudoplatanus* and *B. pendula* but not in *S. aucuparia* (Figure 3c, Figure S4). Similar patterns were observed for the hydraulically-weighted vessel diameter standardized by the distance to the tip ( $D_h^{\text{std}}$ ;

Table S1), which was highly related to  $D_h$  (Figure S5). However, the vessel density (VD) did not change with growing conditions in any of the species (Figure 3d).

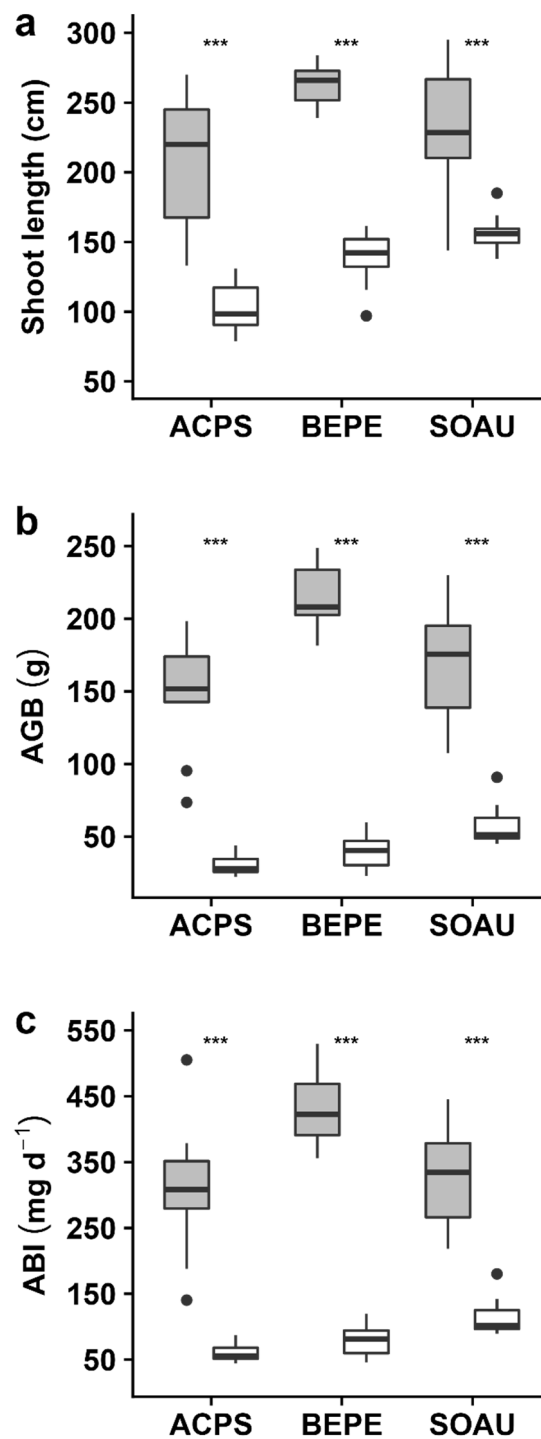


**Figure 2.** Boxplot of growth-related traits of *Acer pseudoplatanus* (ACPS), *Betula pendula* (BEPE), and *Sorbus aucuparia* (SOAU) for the control (grey) and stress (white) treatment. Presented are (a) shoot length, (b) aboveground biomass (AGB), and (c) aboveground biomass increment (ABI). Asterisks indicate the level of significance (\*\*\*,  $p < 0.001$ ; ns, for non-significant).

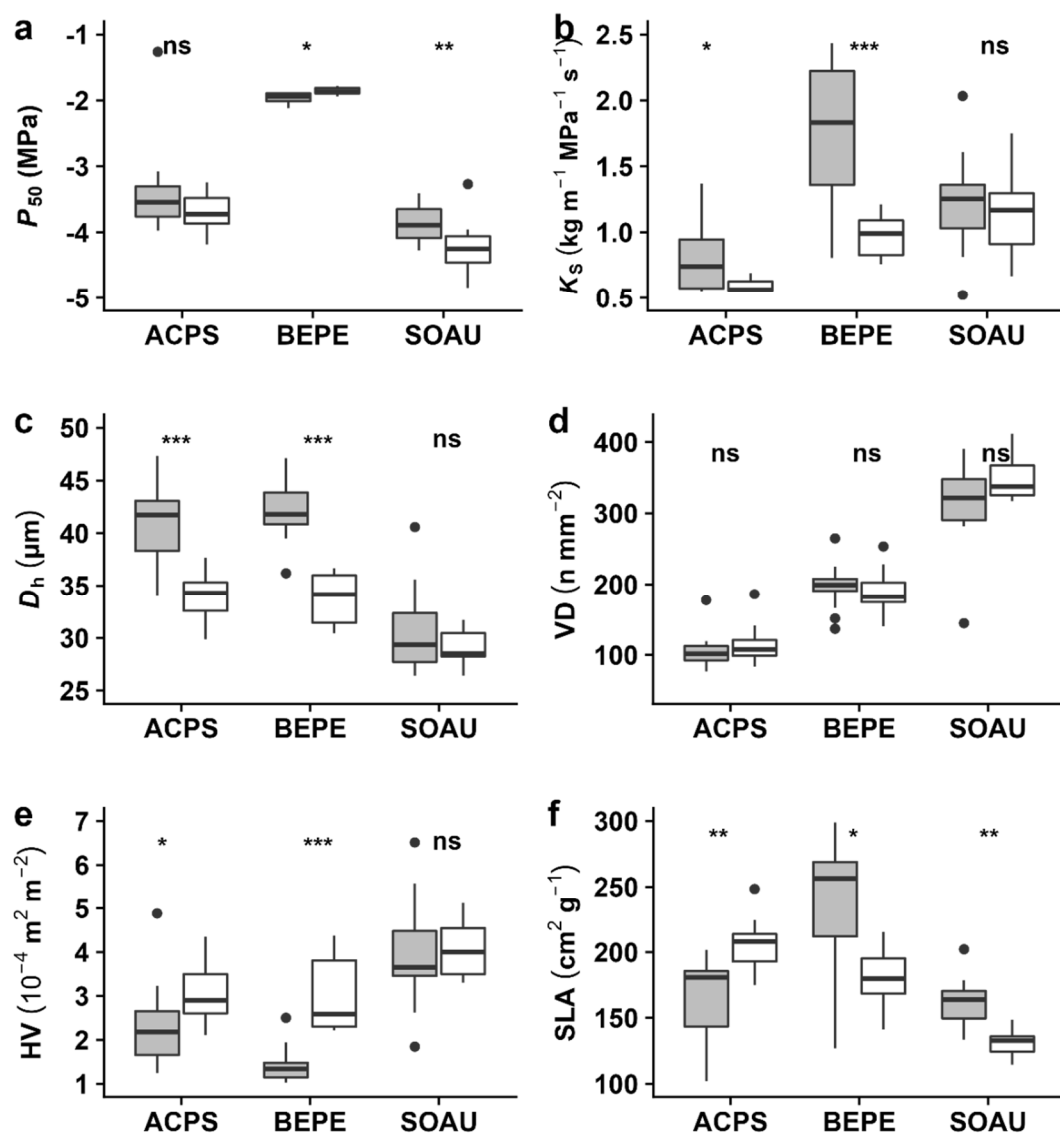


**Figure 3.** Boxplot depicting the variability between treatments for hydraulic, wood anatomical, and leaf morphological traits for the three species. Given are (a) water potential at 50% loss of hydraulic conductivity ( $P_{50}$ ), (b) specific conductivity ( $K_s$ ), (c) hydraulically-weighted vessel diameter ( $D_h$ ), (d) vessel density (VD), (e) Huber value (HV), and (f) specific leaf area (SLA) for the control (grey) and stress (white) treatment. Asterisks indicate the level of significance (\*,  $p < 0.05$ ; \*\*,  $p < 0.01$ ; \*\*\*,  $p < 0.001$ ; ns, for non-significant). For species abbreviations, see Figure 1.

We found significant differences between treatments with regards to leaf characteristics. For example, the specific leaf area (SLA) was lower in the stressed plants of *B. pendula* and *S. aucuparia* compared to the control (Figure 3f), but higher in stressed *A. pseudoplatanus* (Figure 3f). Nonetheless, both *A. pseudoplatanus* and *B. pendula* had a significantly higher Huber value (HV) when stressed (Figure 3e), i.e., a reduced leaf area per cross-sectional sapwood area.

### 3.3. Relationships of Hydraulic Safety-Efficiency, Leaf and Anatomical Traits with Species Growth Performance

In our study, *S. aucuparia* was the most embolism-resistant species with a mean  $P_{50}$  of  $-4.05$  MPa and a mean  $P_{88}$  of  $-5.17$  MPa (Figure 3, Table S1). *A. pseudoplatanus* was found to be less resistant ( $P_{50} = -3.54$  MPa,  $P_{88} = -4.14$  MPa), followed by *B. pendula* ( $P_{50} = -1.91$  MPa,  $P_{88} = -2.14$  MPa). However, *A. pseudoplatanus* was the

least sensitive species regarding the onset of cavitation ( $P_{12} = -2.93$  MPa; Table S1). Although being vulnerable to embolism, *B. pendula* presented the highest hydraulic efficiency ( $K_s = 1.40$  kg m<sup>-1</sup> MPa<sup>-1</sup> s<sup>-1</sup>), followed by *S. aucuparia* (1.18 kg m<sup>-1</sup> MPa<sup>-1</sup> s<sup>-1</sup>) and *A. pseudoplatanus* (0.56 kg m<sup>-1</sup> MPa<sup>-1</sup> s<sup>-1</sup>). Linear regressions depicted significant associations of hydraulic safety with growth traits, although no general trend across species existed (Figure 4a,b). We found that  $P_{50}$  was related to log-transformed ABI in *B. pendula* ( $p < 0.01$ ,  $R^2 = 0.42$ ) and in *S. aucuparia* ( $p < 0.05$ ,  $R^2 = 0.32$ ) but not in *A. pseudoplatanus* (Figure 4a). A positive relationship in *B. pendula* suggests that a higher embolism resistance was associated with a higher growth, while a negative relationship in *S. aucuparia* indicates the opposite, i.e., a low hydraulic safety was related to high growth rates. Similar trends were found between  $P_{50}$  and the shoot length (Figure 4b).

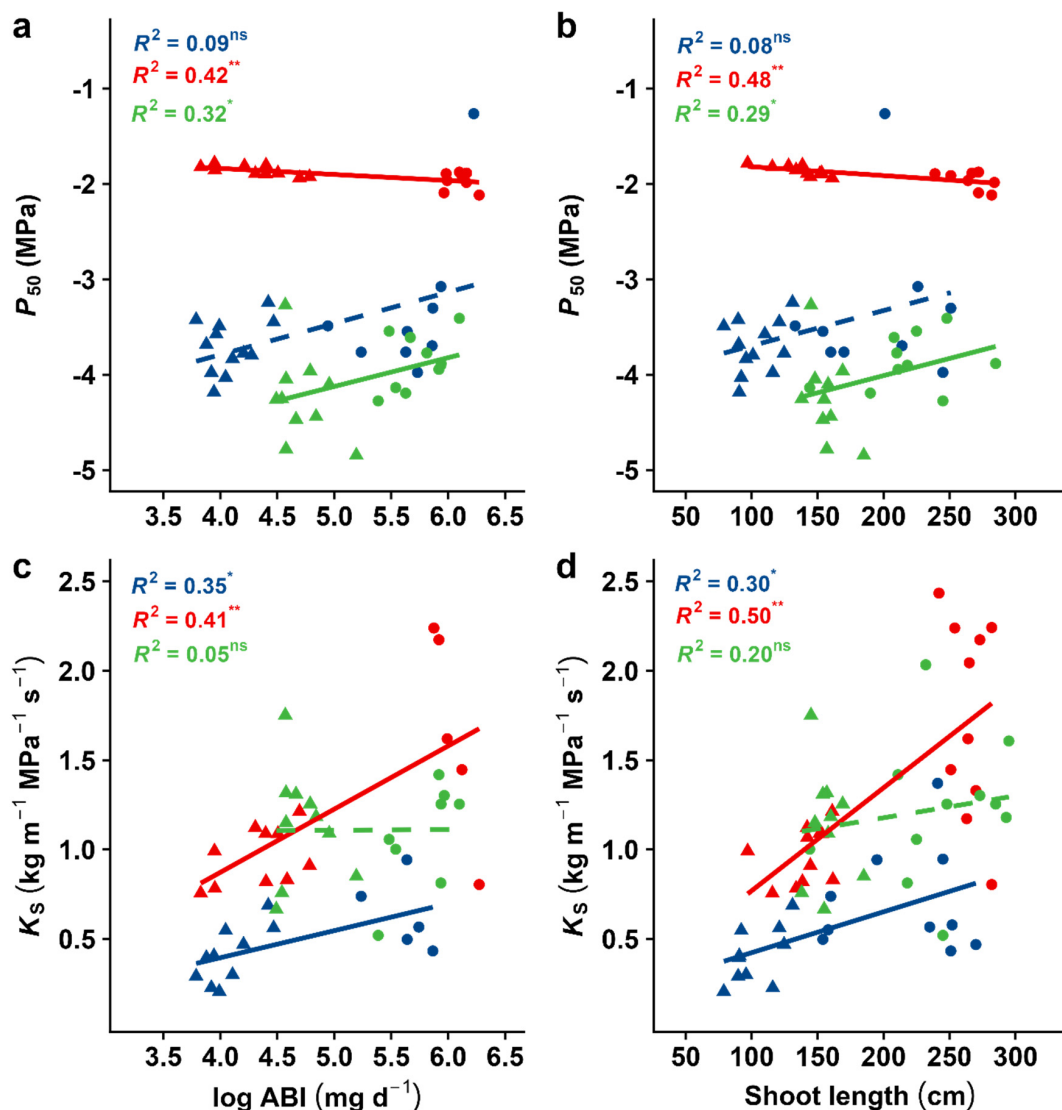


**Figure 4.** Effect of growth performance on the water potential at 50% loss of hydraulic conductivity ( $P_{50}$ ) and specific conductivity ( $K_s$ ). Given are linear regression analyses between (a)  $P_{50}$  or (c)  $K_s$  and log-transformed growth rate, and (b)  $P_{50}$  or (d)  $K_s$  and shoot length. Indicated for each species are the coefficients of determination, i.e., R-squared, for the investigated relationships. Different colours and symbols represent different species and treatments (blue: *A. pseudoplatanus*; red: *B. pendula*; green: *S. aucuparia*; filled circles: control treatment; triangles: stress treatment). Full lines indicate significant effects of variable x on variable y; dashed lines indicate a non-significant relationship. Asterisks indicate the level of significance (\*,  $p < 0.05$ ; \*\*,  $p < 0.01$ ; ns, for non-significant).

In *B. pendula* and *A. pseudoplatanus*, we found that hydraulic conductivity ( $K_S$ ) was significantly affected by growth-related parameters (*B. pendula*:  $p < 0.01$ ,  $R^2 = 0.41$  with ABI and  $p < 0.001$ ,  $R^2 = 0.50$  with shoot length; *A. pseudoplatanus*:  $p < 0.05$ ,  $R^2 = 0.35$  with ABI and  $R^2 = 0.30$  with shoot length; Figure 4c,d). This indicates that a higher hydraulic efficiency was associated with a high juvenile growth. In *S. aucuparia*, on the other hand,  $K_S$  was not related to any of the growth-related variables investigated (Figure 4c,d).

The analysis of other hydraulic efficiency traits ( $K_{pit}$ ) and anatomical traits ( $D_h$  and VD) associated with the growth rate revealed similar contrasting patterns across species (Figure 5). We found that a higher aboveground biomass increment (ABI) was associated with a higher  $K_{pit}$  in *A. pseudoplatanus* and *B. pendula* but not in *S. aucuparia*. Likewise,  $D_h$  was related to higher ABI in *A. pseudoplatanus* and *B. pendula* only. VD, however, was not linked to the growth performance for any of the species (Figure 5c,d). We also found that leaf traits such as the HV were well related to the growth rate in the case of *A. pseudoplatanus* and *B. pendula* but not in *S. aucuparia* (Figure 5f). In the first two species, a lower Huber value was associated with a high growth. The SLA was always related to the ABI, although the nature of the relationship was different across species. *B. pendula* and *S. aucuparia* had a higher SLA associated with a higher growth performance, while the *A. pseudoplatanus* that performed better had a reduced SLA (Figure 5e)

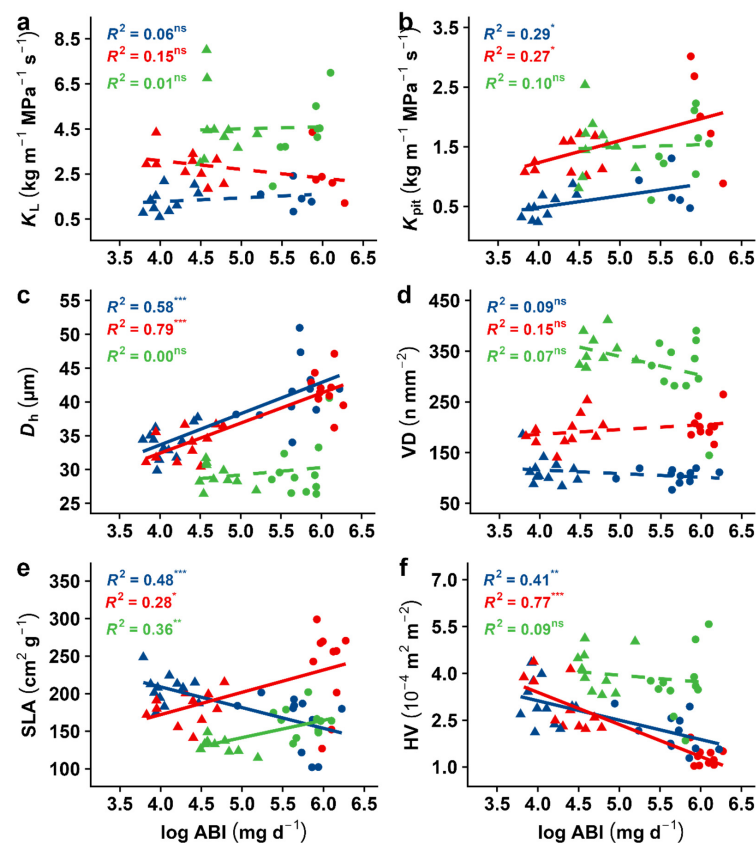


**Figure 5.** Dependency of growth rate on wood anatomical and leaf morphological traits. Given are linear regression analyses of log-transformed growth rate against (a) leaf-specific conductivity ( $K_L$ ), (b) pit conductivity ( $K_{pit}$ ), (c) hydraulically-weighted vessel diameter ( $D_h$ ), (d) vessel density (VD), (e) specific leaf area (SLA), and (f) Huber value (HV). Different colours and symbols represent different species and treatments (blue: *A. pseudoplatanus*; red: *B. pendula*; green: *S. aucuparia*; filled circles: control treatment; triangles: stress treatment). Indicated for each species are the coefficients of determination, i.e., R-squared, for the investigated relationships. Full lines indicate significant effects of variable x on variable y; dashed lines indicate a non-significant relationship. Asterisks indicate the level of significance (\*,  $p < 0.05$ ; \*\*,  $p < 0.01$ ; \*\*\*,  $p < 0.001$ ; ns, for non-significant).

### 3.4. Hydraulic Safety-Efficiency Trade-Offs and Their Relations to Wood Anatomy and Leaf Traits

In all three species, we found that  $P_{50}$  was unrelated to  $K_S$ , indicating the absence of any trade-off between hydraulic safety and efficiency (Figure 6a). As expected from the Hagen–Poiseuille equation,  $K_S$  was well related to  $D_h$  in all species (Figure 6c;  $p < 0.01$  and  $R^2 = 0.35, 0.71$  and  $0.37$  in *A. pseudoplatanus*, *B. pendula*, and *S. aucuparia*, respectively). More interesting was that none of the species showed the relationship between  $D_h$  and  $P_{50}$ , indicating that xylem embolism likely does not depend on vessel diameter in the investigated species of our sample (Figure 6b). We also found that xylem safety was associated with a higher specific leaf area (SLA) in *B. pendula* but a lower one in *S. aucuparia* (Figure S6).

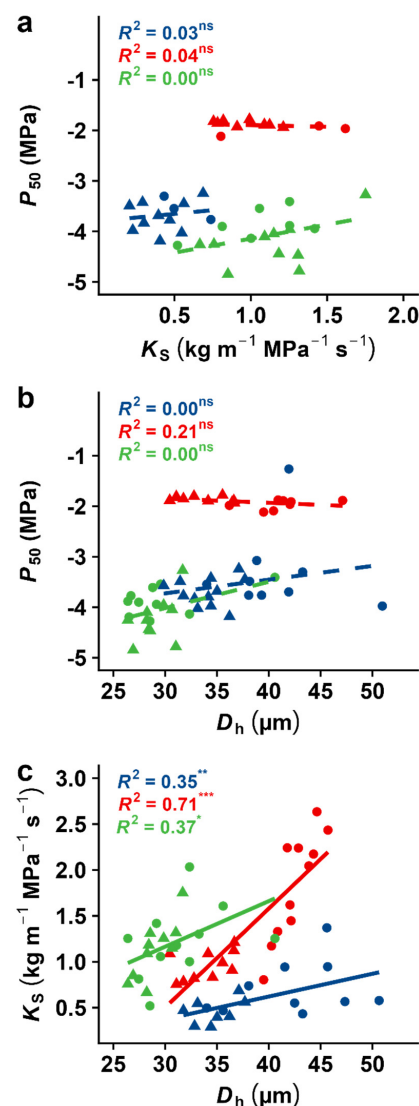


**Figure 6.** Water potential at 50% loss of hydraulic conductivity ( $P_{50}$ ) in relation to (a) specific conductivity ( $K_S$ ) and (b) hydraulically-weighted vessel diameter ( $D_h$ ), as well as (c) specific conductivity ( $K_S$ ) in relation to hydraulically-weighted vessel diameter ( $D_h$ ). The results from the linear regression analyses are given. Different colours and symbols represent different species and treatments (blue: *A. pseudoplatanus*; red: *B. pendula*; green: *S. aucuparia*; filled circles: control treatment; triangles: stress treatment). Indicated for each species are the coefficients of determination, i.e., R-squared, for the investigated relationships. Full lines indicate significant effects of variable x on variable y; dashed lines indicate a non-significant relationship. Asterisks indicate the level of significance (\*,  $p < 0.05$ ; \*\*,  $p < 0.01$ ; \*\*\*,  $p < 0.001$ ; ns, for non-significant).

## 4. Discussion

### 4.1. Relationship of Juvenile Growth with Hydraulic Safety and Efficiency

In our study, significant growth rate and biomass allocation differences were observed for all three species in contrasting growing conditions. We found that juvenile growth was related to either or both hydraulic efficiency and safety in all species. This might suggest a close dependency of juvenile growth on xylem characteristics, but the nature of these relationships contrasted across species. While the growth rate (aboveground biomass increment and shoot length) was negatively related to the xylem pressure at 50% loss of hydraulic conductivity ( $P_{50}$ ) in *B. pendula*, no clear pattern emerged as a positive relationship was found in the case of *S. aucuparia*. However, growth performance was notably associated to a higher hydraulic efficiency in two of the three species, most likely through an increase in hydraulically-weighted vessel diameter ( $D_h$ ), which was strongly and positively related to sapwood-specific hydraulic conductivity ( $K_s$ ). In *B. pendula* and *A. pseudoplatanus*, two species with an isohydric water potential regulation strategy [45,58], and Kumar et al., unpublished, efficiency-related variables (e.g.,  $D_h$  and  $K_s$ ) were associated with higher growth. This is consistent with earlier intra- and inter-specific studies reporting a close association of growth biomass increment to hydraulic efficiency rather than to other wood traits [14,34,37,59]. However, the growth performance was decoupled from hydraulic efficiency in *S. aucuparia*. This was the only species following a rather anisohydric water potential regulation strategy in our study [46], and Kumar et al., unpublished.

In the case of *A. pseudoplatanus*, which has large leaves with a high conductance but a stringent control of its stomates, only hydraulic efficiency and not safety was related to the growth performance. Although *B. pendula* likewise follows an isohydric strategy, a lower embolism resistance was found in stressed individuals with a lower growth performance. In *B. pendula*, no intra-specific variation in  $P_{50}$  has been observed at various stands across Europe, strongly differing in microclimatic conditions [60]. Consequently, we likewise observed a marginal increase in  $P_{50}$  by 0.11 MPa only in *B. pendula*, but counterintuitively plants in the control group developed a slightly more embolism-resistant xylem ( $P_{50} = -1.97$  MPa versus  $-1.86$  MPa, respectively). This might explain why hydraulic safety counterintuitively was negatively, and not positively, related to growth as hypothesized. In the case of *S. aucuparia*, the most embolism-resistant species with the least stringent stomatal control, we found that hydraulic safety was positively associated with growth as speculated, i.e., fast-growing individuals developed a less embolism-resistant xylem ( $P_{50} = -3.87$  MPa versus  $-4.24$  MPa in the control versus the stress treatment, respectively). The disparities in the growth–hydraulic safety trade-off between species observed here was also reported in previous studies. While a negative relationship was found for willow genotypes [28,41] and provenances of cedar [61], a positive relationship was reported for poplar hybrids [38] and European beech [62], and other studies did not find any link at all [14,22,24,33,39].

Contrasting results across studies suggest that relationships between growth performance and hydraulic safety, but also efficiency, do not necessarily present a general trend across species but may be linked to species-specific hydraulic strategies [63].

### 4.2. Relationship of Juvenile Growth with Leaf-Related Traits

Leaf traits are often used as an indicator of plant growth performance since they are responsive to the local environment [64,65]. For example, the specific leaf area (SLA) is often assumed to be a central trait under species-selection, and species with large and thin but short-lived leaves tend to have a resource-acquisition strategy based on a quick return on leaf investments [66,67]. In this study, we found the SLA to be linked to growth performance, but once more without revealing any clear trend. While we found that a reduction of SLA was associated with a higher growth performance in *A. pseudoplatanus*, the opposite was found in the other two species. In our study, stressed individuals of *A. pseudoplatanus* developed larger and/or lighter leaves compared to the control, although the opposite relationship is usually associated with environmental stress [68,69].

We also found that two of the three species, namely *A. pseudoplatanus* and *B. pendula*, had Huber values (HV), i.e., the sapwood-to-leaf area ratios, that decreased with the growth performance as one would expect. While the third species, *S. aucuparia*, showed the same tendency, this relationship was non-significant. Thus, all species of our sample adjusted their leaf-level water supply in response to more stressful climatic conditions by reducing the size of single leaves (Table S1), and potentially their numbers. Our results suggest that all three foliar traits covered are highly plastic and responsive to climatic stress conditions, consistent with studies reporting that leaf traits respond to gradients of water availability [32,65].

#### 4.3. Trade-Off between Hydraulic Efficiency and Safety and Anatomic Determinants

In agreement with a growing body of evidence, we did not find any relationship between the hydraulic safety and efficiency across the three species of our sample cf. [55,70,71], but see [22]. Although we only investigated siblings originating from the same parental tree, our results support the assumption that different evolutionary pathways exist for achieving xylem safety and efficiency, and that the safety–efficiency trade-off may be species- and scale-dependent [17,71]. Furthermore, hydraulic safety appears to be a rather conservative trait in temperate broad-leaved tree species cf. [72,73], while hydraulic efficiency is more plastic in order to meet the water demand of the supported foliage at the place of growth.

Therefore, the majority of recent results support a divergence from the classical paradigm of plant hydraulics, postulating that plant hydraulic functioning is dependent on a trade-off between xylem safety and efficiency [74]. It is evident that some species might have both a low safety and a low efficiency, which means that the anatomical basis for a high efficiency could be trading off with traits other than embolism resistance [20]. Hence, a question arises on the significance of given anatomical features that play a role. On that matter, the vessel diameter was initially proposed as the primary anatomical determinant of the safety–efficiency trade-off since vessel conductivity increases in the proportion of its diameter at the fourth power according to the Hagen–Poiseuille equation [75]. This is supported by our study, as  $D_h$  was related to  $K_S$  in all three species. However, it seems that vessel diameter is not universally linked to embolism resistance. While several studies observed a dependency of  $P_{50}$  on  $D_h$  within or across species [13–15,19,39], others could not [24,38,40,76,77]. It is meanwhile well-established that embolism resistance is only indirectly related to vessel diameter through an increased number of interconnected vessels, while it is directly related to pit membrane thickness [12]. Thus, the focus has shifted from conduit diameter to inter-vessel transport and pit membrane characteristics such as pore size and membrane thickness for determining embolism resistance. Further work is needed to shed light on these controversies.

#### 4.4. Variability in Hydraulic and Foliar Traits in Response to Environmental Stress

As shown and discussed, the three species exhibited significant differences in their hydraulic and leaf functional attributes between both treatments. Because genetic material was similar within a species, those differences can be imputed to a plastic response of the plants to heat stress. Knowledge of the degree of phenotypic plasticity of given traits is essential to better understand tree responses to climate change. In *B. pendula*, the highest degree of variability was found. Here, 14 of the 17 growth-related, wood anatomical, hydraulic, and leaf morphological traits differed between treatments, while only six differed in the case of *S. aucuparia* (Table S1). Although stressed plants of *S. aucuparia* developed a more embolism-resistant xylem, other traits such as hydraulic efficiency and its main anatomical determinant, vessel diameter, were unaffected by the growing conditions. Because *S. aucuparia* relies on its high resistance to embolism to survive drought, this might explain why mainly xylem safety responded plastically. In *B. pendula*, on the other hand, both embolism resistance and specific conductivity decreased in stressed plants. This was associated with a reduction in the vessel diameter, and this effect remained even after standardizing for the distance to the tip (Table S1). Altogether, this matches the

expected growth strategy of this pioneer tree species. In *A. pseudoplatanus*, we found a strong reduction of hydraulic conductivity and vessel diameter but not xylem safety. This species seems to have a stringent stomatal control [Kumar et al., unpublished] associated with a fairly embolism-resistant xylem.

## 5. Conclusions

This study on the association of juvenile growth with xylem safety and efficiency revealed considerable inter-specific differences. The distinguishable relationships across species could be related to their habitat preferences and ecological strategies. We found species-specific links between growth performances and hydraulic safety and efficiency in two of the tree species but without revealing any clear pattern. The safety-related traits appeared more static, while efficiency traits revealed a higher intra-specific plasticity. In all species, the hydraulic efficiency was strongly dependent on vessel diameter but was unrelated to xylem safety. Overall, understanding the links among hydraulic traits and their specific association with juvenile growth performance during stress is necessary to understand plant behaviour in a warmer and drier environment and to improve breeding programs.

**Supplementary Materials:** The following supporting information can be downloaded at: <https://www.mdpi.com/article/10.3390/f13060909/s1>, Table S1: Summary of all major variables estimated on the three temperate tree species; Figure S1: Daily maximum temperature and vapour pressure deficit outside and inside a climate chamber during the growing season from May to September 2022; Figure S2: Daily maximum temperature and vapour pressure deficit outside and inside a climate chamber during 2019 and 2020 growing seasons; Figure S3: Boxplot depicting the plasticity of additional safety—efficiency traits for the three tree species; Figure S4: Cross-sectional images of stem wood of the three tree species as well as vessel size classes contribution to Khtheo; Figure S5: Standardized vessel diameter (Dhstd) in relation to hydraulically—weighted vessel diameter (Dh) of the three temperate tree species; Figure S6: Water potential at 50% loss of hydraulic conductivity (P50) and specific conductivity (KS) in relation to specific leaf area (SLA) of the three temperate tree species.

**Author Contributions:** B.S. designed the study, M.K. and S.S.P. performed all measurements, and M.K. carried out the statistical analyses in close collaboration with P.-A.W., M.K. and P.-A.W. wrote the first version of the manuscript, which was intensively discussed and revised by all authors. All authors have read and agreed to the published version of the manuscript.

**Funding:** This work was financially supported by the Indian Council of Agricultural Research (ICAR), New Delhi, India, through the Netaji Subhash-ICAR International Fellowship granted to Manish Kumar (F.No.: 18(20)/2018-EQR/Edn).

**Data Availability Statement:** All data used in this manuscript are present in the manuscript and its supporting information.

**Acknowledgments:** This publication was supported by the Open Access Publication Fund of the University of Würzburg. The first author gratefully acknowledges the financial support provided by the Indian Council of Agricultural Research (ICAR), New Delhi, India, through the Netaji Subhash-ICAR International Fellowship for his doctoral programme. The logistical and scientific assistance received from the University of Würzburg, Germany, is gratefully acknowledged. Additionally, we thank Roman Mathias Link for his guidance with statistical analysis. Special thanks to Christine Gernert and Yvonne Heppenstiel for their skillful support in preparing transverse sections and microscopic work for wood anatomy, and to Jutta Winkler-Steinbeck for taking care of the plants.

**Conflicts of Interest:** The authors declare no conflict of interest.

## References

1. IPCC. Climate Change: The Physical Science Basis. In *Contribution of Working Group I to the Sixth Assessment Report of the Intergovernmental Panel on Climate Change*; Masson-Delmotte, V., Zhai, A.P., Pirani, S.L., Connors, C., Péan, S., Berger, N., Caud, Y., Chen, L., Goldfarb, M.I., Gomis, M., et al., Eds.; Cambridge University Press: Cambridge, UK, 2021.
2. Eziz, A.; Yan, Z.; Tian, D.; Han, W.; Tang, Z.; Fang, J. Drought effect on plant biomass allocation: A meta-analysis. *Ecol. Evol.* **2017**, *7*, 11002–11010. [[CrossRef](#)]

3. McDowell, N.; Pockman, W.T.; Allen, C.D.; Breshears, D.D.; Cobb, N.; Kolb, T.; Plaut, J.; Sperry, J.; West, A.; Williams, D.G.; et al. Mechanisms of plant survival and mortality during drought: Why do some plants survive while others succumb to drought? *New Phytol.* **2008**, *178*, 719–739. [[CrossRef](#)] [[PubMed](#)]
4. Rowland, L.; da Costa, A.C.L.; Galbraith, D.R.; Oliveira, R.S.; Binks, O.J.; Oliveira, A.A.R.; Pullen, A.M.; Doughty, C.E.; Metcalfe, D.B.; Vasconcelos, S.S.; et al. Death from drought in tropical forests is triggered by hydraulics not carbon starvation. *Nature* **2015**, *528*, 119–122. [[CrossRef](#)] [[PubMed](#)]
5. Clark, J.S.; Iverson, L.; Woodall, C.W.; Allen, C.D.; Bell, D.; Bragg, D.C.; D’Amato, A.W.; Davis, F.; Hersh, M.; Ibanez, I.; et al. The impacts of increasing drought on forest dynamics, structure, and biodiversity in the United States. *Glob. Chang. Biol.* **2016**, *22*, 2329–2352. [[CrossRef](#)] [[PubMed](#)]
6. Choat, B.; Brodribb, T.J.; Brodersen, C.R.; Duursma, R.A.; López, R.; Medlyn, B.E. Triggers of Tree Mortality under Drought. *Nature* **2018**, *558*, 531–539. [[CrossRef](#)]
7. Duursma, R.A.; Blackman, C.J.; López, R.; Martin-StPaul, N.K.; Cochard, H.; Medlyn, B.E. On the minimum leaf conductance: Its role in models of plant water use, and ecological and environmental controls. *New Phytol.* **2019**, *221*, 693–705. [[CrossRef](#)] [[PubMed](#)]
8. Britton, T.G.; Brodribb, T.J.; Richards, S.A.; Ridley, C.; Hovenden, M.J. Canopy damage during a natural drought depends on species identity, physiology and stand composition. *New Phytol.* **2022**, *233*, 2058–2070. [[CrossRef](#)] [[PubMed](#)]
9. Hajek, P.; Link, R.M.; Nock, C.; Bauhus, J.; Gebauer, T.; Gessler, A.; Kovach, K.; Messier, C.; Paquette, A.; Saurer, M.; et al. Mutually inclusive mechanisms of drought-induced tree mortality. *Glob. Change Biol.* **2022**, *28*, 3365–3378. [[CrossRef](#)]
10. Nolan, R.H.; Gauthey, A.; Lasso, A.; Medlyn, B.E.; Smith, R.; Chhajed, S.S.; Fuller, K.; Song, M.; Li, X.; Beaumont, L.J.; et al. Hydraulic failure and tree size linked with canopy die-back in eucalypt forest during extreme drought. *New Phytol.* **2021**, *230*, 1354–1365. [[CrossRef](#)]
11. Li, S.; Lens, F.; Espino, S.; Karimi, Z.; Klepsch, M.; Schenk, H.J.; Schmitt, M.; Schuldt, B.; Jansen, S. Intervessel pit membrane thickness as a key determinant of embolism resistance in angiosperm xylem. *IAWA J.* **2016**, *37*, 152–171. [[CrossRef](#)]
12. Kaack, L.; Weber, M.; Isasa, E.; Karimi, Z.; Li, S.; Pereira, L.; Trabi, C.L.; Zhang, Y.; Schenk, H.J.; Schuldt, B.; et al. Pore constrictions in intervessel pit membranes provide a mechanistic explanation for xylem embolism resistance in angiosperms. *New Phytol.* **2021**, *230*, 1829–1843. [[CrossRef](#)] [[PubMed](#)]
13. Awad, H.; Barigah, T.; Badel, E.; Cochard, H.; Herbette, S. Poplar vulnerability to xylem cavitation acclimates to drier soil conditions. *Physiol. Plant.* **2010**, *139*, 280–288. [[CrossRef](#)] [[PubMed](#)]
14. Hajek, P.; Leuschner, C.; Hertel, D.; Delzon, S.; Schuldt, B. Trade-offs between xylem hydraulic properties, wood anatomy and yield in *Populus*. *Tree Physiol.* **2014**, *34*, 744–756. [[CrossRef](#)] [[PubMed](#)]
15. Maherali, H.; Moura, C.F.; Caldeira, M.C.; Willson, C.J.; Jackson, R.B. Functional coordination between leaf gas exchange and vulnerability to xylem cavitation in temperate forest trees. *Plant Cell Environ.* **2006**, *29*, 571–583. [[CrossRef](#)]
16. Domec, J.; King, J.S.; Noormets, A.; Treasure, E.; Gavazzi, M.J.; Sun, G.; McNulty, S.G. Hydraulic redistribution of soil water by roots affects whole-stand evapotranspiration and net ecosystem carbon exchange. *New Phytol.* **2010**, *187*, 171–183. [[CrossRef](#)]
17. Isasa, E.; Link, R.; Jansen, S.; Sarmento Cabral, J.; Schuldt, B. Addressing Controversies in Safety-Vessel Diameter Relationships; In Proceedings of the Conference Ecology Across Borders 2021, Liverpool, UK, 12–15 December 2021. [[CrossRef](#)]
18. Sperry, J.S.; Tyree, M.T. Water-stress-induced xylem embolism in three species of conifers. *Plant Cell Environ.* **1990**, *13*, 427–436. [[CrossRef](#)]
19. Hacke, U.G.; Sperry, J.S.; Wheeler, J.K.; Castro, L. Scaling of angiosperm xylem structure with safety and efficiency. *Tree Physiol.* **2006**, *26*, 689–701. [[CrossRef](#)]
20. Gleason, S.M.; Westoby, M.; Jansen, S.; Choat, B.; Hacke, U.; Pratt, R.B.; Bhaskar, R.; Brodribb, T.; Bucci, S.J.; Cao, K.-F.; et al. Weak tradeoff between xylem safety and xylem-specific hydraulic efficiency across the world’s woody plant species. *New Phytol.* **2016**, *209*, 123–136. [[CrossRef](#)]
21. Choat, B.; Jansen, S.; Brodribb, T.J.; Cochard, H.; Delzon, S.; Bhaskar, R.; Bucci, S.J.; Feild, T.S.; Gleason, S.M.; Hacke, U.G.; et al. Global convergence in the vulnerability of forests to drought. *Nature* **2012**, *491*, 752–755. [[CrossRef](#)]
22. Schumann, K.; Leuschner, C.; Schuldt, B. Xylem hydraulic safety and efficiency in relation to leaf and wood traits in three temperate *Acer* species differing in habitat preferences. *Trees* **2019**, *33*, 1475–1490. [[CrossRef](#)]
23. Liu, H.; Ye, Q.; Gleason, S.M.; He, P.; Yin, D. Weak tradeoff between xylem hydraulic efficiency and safety: Climatic seasonality matters. *New Phytol.* **2021**, *229*, 1440–1452. [[CrossRef](#)] [[PubMed](#)]
24. Schuldt, B.; Knutzen, F.; Delzon, S.; Jansen, S.; Müller-Haubold, H.; Burlett, R.; Clough, Y.; Leuschner, C. How adaptable is the hydraulic system of European beech in the face of climate change-related precipitation reduction? *New Phytol.* **2016**, *210*, 443–458. [[CrossRef](#)] [[PubMed](#)]
25. Brodribb, T.J. Xylem hydraulic physiology: The functional backbone of terrestrial plant productivity. *Plant Sci.* **2009**, *177*, 245–251. [[CrossRef](#)]
26. Tyree, M.T. Hydraulic limits on tree performance: Transpiration, carbon gain and growth of trees. *Trees* **2003**, *17*, 95–100. [[CrossRef](#)]
27. Domec, J.-C.; Gartner, B.L. Relationship between growth rates and xylem hydraulic characteristics in young, mature and old-growth ponderosa pine trees. *Plant Cell Environ.* **2003**, *26*, 471–483. [[CrossRef](#)]

28. Wikberg, J.; Ögren, E. Interrelationships between water use and growth traits in biomass-producing willows. *Trees Struct. Funct.* **2004**, *18*, 70–76. [[CrossRef](#)]
29. Zhang, J.-L.; Cao, K.-F. Stem hydraulics mediates leaf water status, carbon gain, nutrient use efficiencies and plant growth rates across dipterocarp species. *Funct. Ecol.* **2009**, *23*, 658–667. [[CrossRef](#)]
30. Fichot, R.; Chamaillard, S.; Depardieu, C.; Le Thiec, D.; Cochard, H.; Barigah, T.S.; Brignolas, F. Hydraulic efficiency and coordination with xylem resistance to cavitation, leaf function, and growth performance among eight unrelated *Populus deltoides* × *Populus nigra* hybrids. *J. Exp. Bot.* **2011**, *62*, 2093–2106. [[CrossRef](#)]
31. Fan, Z.-X.; Zhang, S.-B.; Hao, G.-Y.; Ferry Slik, J.W.; Cao, K.-F. Hydraulic conductivity traits predict growth rates and adult stature of 40 Asian tropical tree species better than wood density. *J. Ecol.* **2012**, *100*, 732–741. [[CrossRef](#)]
32. Gleason, S.M.; Butler, D.W.; Ziemińska, K.; Waryszak, P.; Westoby, M. Stem xylem conductivity is key to plant water balance across Australian angiosperm species. *Funct. Ecol.* **2012**, *26*, 343–352. [[CrossRef](#)]
33. Guet, J.; Fichot, R.; Lédée, C.; Laurans, F.; Cochard, H.; Delzon, S.; Bastien, C.; Brignolas, F. Stem xylem resistance to cavitation is related to xylem structure but not to growth and water-use efficiency at the within-population level in *Populus nigra* L. *J. Exp. Bot.* **2015**, *66*, 4643–4652. [[CrossRef](#)] [[PubMed](#)]
34. Hoerber, S.; Leuschner, C.; Köhler, L.; Arias-Aguilar, D.; Schuldt, B. The importance of hydraulic conductivity and wood density to growth performance in eight tree species from a tropical semi-dry climate. *For. Ecol. Manag.* **2014**, *330*, 126–136. [[CrossRef](#)]
35. Eller, C.B.; Bittencourt, P.R.L.; Oliveira, R.S. Using sap flow to measure whole-tree hydraulic conductance loss in response to drought. *Acta Hort.* **2018**, *1222*, 75–84. [[CrossRef](#)]
36. Gleason, S.M.; Stephens, A.E.A.; Tozer, W.C.; Blackman, C.J.; Butler, D.W.; Chang, Y.; Cook, A.M.; Cooke, J.; Laws, C.A.; Rosell, J.A.; et al. Shoot growth of woody trees and shrubs is predicted by maximum plant height and associated traits. *Funct. Ecol.* **2018**, *32*, 247–259. [[CrossRef](#)]
37. Kotowska, M.M.; Link, R.M.; Röhl, A.; Hertel, D.; Hölscher, D.; Waite, P.-A.; Moser, G.; Tjoa, A.; Leuschner, C.; Schuldt, B. Effects of Wood Hydraulic Properties on Water Use and Productivity of Tropical Rainforest Trees. *Front. For. Glob. Chang.* **2021**, *3*, 598759. [[CrossRef](#)]
38. Fichot, R.; Barigah, T.S.; Chamaillard, S.; Le Thiec, D.; Laurans, F.; Cochard, H.; Brignolas, F. Common trade-offs between xylem resistance to cavitation and other physiological traits do not hold among unrelated *Populus deltoides* × *Populus nigra* hybrids: Xylem resistance to cavitation and water relations in poplar. *Plant Cell Environ.* **2010**, *33*, 1553–1568. [[CrossRef](#)]
39. Sterck, F.J.; Martínez-Vilalta, J.; Mencuccini, M.; Cochard, H.; Gerrits, P.; Zweifel, R.; Herrero, A.; Korhonen, J.F.; Llorens, P.; Nikinmaa, E.; et al. Understanding trait interactions and their impacts on growth in Scots pine branches across Europe: Functional branch trait coordination. *Funct. Ecol.* **2012**, *26*, 541–549. [[CrossRef](#)]
40. Hajek, P.; Kurjak, D.; von Wühlisch, G.; Delzon, S.; Schuldt, B. Intraspecific Variation in Wood Anatomical, Hydraulic, and Foliar Traits in Ten European Beech Provenances Differing in Growth Yield. *Front. Plant Sci.* **2016**, *7*, 791. [[CrossRef](#)]
41. Cochard, H.; Casella, E.; Mencuccini, M. Xylem vulnerability to cavitation varies among poplar and willow clones and correlates with yield. *Tree Physiol.* **2007**, *27*, 1761–1767. [[CrossRef](#)]
42. Ellenberg, H.; Leuschner, C. Vegetation Mitteleuropas mit den Alpen. In *Ökologischer, Dynamischer und Historischer Sicht*; Utb GmbH: Stuttgart, Germany, 2010.
43. Robson, T.M.; Hartikainen, S.M.; Aphalo, P.J. How Does Solar Ultraviolet-B Radiation Improve Drought Tolerance of Silver Birch (*Betula Pendula* Roth.) Seedlings? *Plant Cell Environment* **2015**, *38*, 953–967. [[CrossRef](#)]
44. Leuschner, C.; Meier, I.C. The ecology of Central European tree species: Trait spectra, functional trade-offs, and ecological classification of adult trees. *Perspect. Plant Ecol. Evol. Syst.* **2018**, *33*, 89–103. [[CrossRef](#)]
45. Leuschner, C.; Wedde, P.; Lübke, T. The relation between pressure—Volume curve traits and stomatal regulation of water potential in five temperate broadleaf tree species. *Ann. For. Sci.* **2019**, *76*, 60. [[CrossRef](#)]
46. Vogt, U.K. Hydraulic vulnerability, vessel refilling, and seasonal courses of stem water potential of *Sorbus aucuparia* L. and *Sambucus nigra* L. *J. Exp. Bot.* **2001**, *52*, 1527–1536. [[CrossRef](#)] [[PubMed](#)]
47. Hari, V.; Rakovec, O.; Markonis, Y.; Hanel, M.; Kumar, R. Increased future occurrences of the exceptional 2018–2019 Central European drought under global warming. *Sci. Rep.* **2020**, *10*, 12207. [[CrossRef](#)] [[PubMed](#)]
48. Torres-Ruiz, J.M.; Jansen, S.; Choat, B.; McElrone, A.J.; Cochard, H.; Brodribb, T.J.; Badel, E.; Burrell, R.; Bouche, P.S.; Brodersen, C.R.; et al. Direct X-ray Microtomography Observation Confirms the Induction of Embolism upon Xylem Cutting under Tension. *Plant Physiol.* **2015**, *167*, 40–43. [[CrossRef](#)] [[PubMed](#)]
49. Cochard, H.; Damour, G.; Bodet, C.; Tharwat, I.; Poirier, M.; Améglio, T. Evaluation of a new centrifuge technique for rapid generation of xylem vulnerability curves. *Physiol. Plant.* **2005**, *124*, 410–418. [[CrossRef](#)]
50. Pammenter, N.W.; Van der Willigen, C. A mathematical and statistical analysis of the curves illustrating vulnerability of xylem to cavitation. *Tree Physiol.* **1998**, *18*, 589–593. [[CrossRef](#)]
51. White, F.M. *Viscous Fluid Flow*; McGraw-Hill: New York, NY, USA, 1991.
52. Sperry, J.S.; Nichols, K.L.; Sullivan, J.E.M.; Eastlack, S.E. Xylem Embolism in Ring-Porous, Diffuse-Porous, and Coniferous Trees of Northern Utah and Interior Alaska. *Ecology* **1994**, *75*, 1736–1752. [[CrossRef](#)]
53. Anfodillo, T.; Petit, G.; Crivellaro, A. Axial conduit widening in woody species: A still neglected anatomical pattern. *IAWA J.* **2013**, *34*, 352–364. [[CrossRef](#)]

54. West, G.B.; Brown, J.H.; Enquist, B.J. A general model for the structure and allometry of plant vascular systems. *Nature* **1999**, *400*, 664–667. [[CrossRef](#)]
55. Larter, M.; Pfautsch, S.; Domec, J.-C.; Trueba, S.; Nagalingum, N.; Delzon, S. Aridity drove the evolution of extreme embolism resistance and the radiation of conifer genus *Callitris*. *New Phytol.* **2017**, *215*, 97–112. [[CrossRef](#)] [[PubMed](#)]
56. R Core Team. *R: A Language and Environment for Statistical Computing*; R Core Team: Vienna, Austria, 2020.
57. Wickham, H.; Averick, M.; Bryan, J.; Chang, W.; McGowan, L.D.; François, R.; Grolemund, G.; Hayes, A.; Henry, L.; Hester, J.; et al. Welcome to the Tidyverse. *J. Open Source Softw.* **2019**, *4*, 1686. [[CrossRef](#)]
58. Beikircher, B.; Sack, L.; Ganthaler, A.; Losso, A.; Mayr, S. Hydraulic-stomatal coordination in tree seedlings: Tight correlation across environments and ontogeny in *Acer pseudoplatanus*. *New Phytol.* **2021**, *232*, 1297–1310. [[CrossRef](#)]
59. Kotowska, M.M.; Hertel, D.; Rajab, Y.A.; Barus, H.; Schuldt, B. Patterns in hydraulic architecture from roots to branches in six tropical tree species from cacao agroforestry and their relation to wood density and stem growth. *Front. Plant Sci.* **2015**, *6*, 191. [[CrossRef](#)] [[PubMed](#)]
60. González-Muñoz, N.; Sterck, F.; Torres-Ruiz, J.M.; Petit, G.; Cochard, H.; von Arx, G.; Lintunen, A.; Caldeira, M.C.; Capdeville, G.; Copini, P.; et al. Quantifying in situ phenotypic variability in the hydraulic properties of four tree species across their distribution range in Europe. *PLoS ONE* **2018**, *13*, e0196075. [[CrossRef](#)] [[PubMed](#)]
61. Ducrey, M.; Huc, R.; Ladjal, M.; Guehl, J.-M. Variability in growth, carbon isotope composition, leaf gas exchange and hydraulic traits in the eastern Mediterranean cedars *Cedrus libani* and *C. brevifolia*. *Tree Physiol.* **2008**, *28*, 689–701. [[CrossRef](#)]
62. Herbette, S.; Charrier, O.; Cochard, H.; Barigah, T.S. Delayed effect of drought on xylem vulnerability to embolism in *Fagus sylvatica*. *Can. J. For. Res.* **2020**, *51*, 622–626. [[CrossRef](#)]
63. Hartmann, H.; Link, R.M.; Schuldt, B. A whole-plant perspective of isohydry: Stem-level support for leaf-level plant water regulation. *Tree Physiol.* **2021**, *41*, 901–905. [[CrossRef](#)]
64. Chaturvedi, R.K.; Raghubanshi, A.S.; Singh, J.S. Growth of tree seedlings in a tropical dry forest in relation to soil moisture and leaf traits. *J. Plant Ecol.* **2013**, *6*, 158–170. [[CrossRef](#)]
65. Weithmann, G.; Schuldt, B.; Link, R.M.; Heil, D.; Hoerber, S.; John, H.; Müller-Haubold, H.; Schüller, L.; Schumann, K.; Leuschner, C. Leaf trait modification in European beech trees in response to climatic and edaphic drought. *Plant Biol.* **2021**. [[CrossRef](#)]
66. Markesteijn, L.; Poorter, L.; Bongers, F.; Paz, H.; Sack, L. Hydraulics and life history of tropical dry forest tree species: Coordination of species' drought and shade tolerance. *New Phytol.* **2011**, *191*, 480–495. [[CrossRef](#)] [[PubMed](#)]
67. Schreiber, S.G.; Hacke, U.G.; Chamberland, S.; Lowe, C.W.; Kamelchuk, D.; Braeutigam, K.; Campbell, M.; Thomas, B.R. Leaf size serves as a proxy for xylem vulnerability to cavitation in plantation trees. *Plant Cell Environ.* **2016**, *39*, 272–281. [[CrossRef](#)] [[PubMed](#)]
68. Cunningham, S.A.; Summerhayes, B.; Westoby, M. Evolutionary divergences in leaf structure and chemistry, comparing rainfall and soil nutrient gradients. *Ecol. Monogr.* **1999**, *69*, 569–588. [[CrossRef](#)]
69. Wright, I.J.; Reich, P.B.; Westoby, M.; Ackerly, D.D.; Baruch, Z.; Bongers, F.; Cavender-Bares, J.; Chapin, T.; Cornelissen, J.H.C.; Diemer, M.; et al. The worldwide leaf economics spectrum. *Nature* **2004**, *428*, 821–827. [[CrossRef](#)]
70. Torres-Ruiz, J.M.; Cochard, H.; Fonseca, E.; Badel, E.; Gazarini, L.; Vaz, M. Differences in functional and xylem anatomical features allow *Cistus* species to co-occur and cope differently with drought in the Mediterranean region. *Tree Physiol.* **2017**, *37*, 755–766. [[CrossRef](#)] [[PubMed](#)]
71. Lübke, T.; Lamarque, L.J.; Delzon, S.; Ruiz, J.M.T.; Burlett, R.; Leuschner, C.; Schuldt, B. High variation in hydraulic efficiency but not xylem safety between roots and branches in four temperate broad-leaved tree species. *Funct. Ecol.* **2022**, *36*, 699–712. [[CrossRef](#)]
72. Rosas, T.; Mencuccini, M.; Barba, J.; Cochard, H.; Saura-Mas, S.; Martínez-Vilalta, J. Adjustments and coordination of hydraulic, leaf and stem traits along a water availability gradient. *New Phytol.* **2019**, *223*, 632–646. [[CrossRef](#)]
73. Fuchs, S.; Schuldt, B.; Leuschner, C. Identification of drought-tolerant tree species through climate sensitivity analysis of radial growth in Central European mixed broadleaf forests. *For. Ecol. Manag.* **2021**, *494*, 119287. [[CrossRef](#)]
74. Tyree, M.T.; Davis, S.D.; Cochard, H. Biophysical Perspectives of Xylem Evolution: Is there a Tradeoff of Hydraulic Efficiency for Vulnerability to Dysfunction? *IAWA J.* **1994**, *15*, 335–360. [[CrossRef](#)]
75. Tyree, M.T.; Zimmermann, M.H. Hydraulic Architecture of Woody Shoots. In *Xylem Structure and the Ascent of Sap*; Tyree, M.T., Zimmermann, M.H., Eds.; Springer: Berlin/Heidelberg, Germany, 2002; pp. 143–174.
76. Choat, B.; Cobb, A.R.; Jansen, S. Structure and function of bordered pits: New discoveries and impacts on whole-plant hydraulic function. *New Phytol.* **2008**, *177*, 608–626. [[CrossRef](#)]
77. Lens, F.; Sperry, J.S.; Christman, M.A.; Choat, B.; Rabaey, D.; Jansen, S. Testing hypotheses that link wood anatomy to cavitation resistance and hydraulic conductivity in the genus *Acer*. *New Phytol.* **2011**, *190*, 709–723. [[CrossRef](#)] [[PubMed](#)]